RESEARCH ARTICLE

Contact values for disparate-size hard-sphere mixtures

Andrés Santos[a]*, Santos B. Yuste[a], Mariano López de Haro[a†],
Morad Alawneh[b] and Douglas Henderson[b]

*[a]Departamento de Física, Universidad de Extremadura, E-06071 Badajoz,
Spain; [b]Department of Chemistry and Biochemistry, Brigham Young University,
Provo, UT 84602-5700, USA*

A universality ansatz for the contact values of a multicomponent mixture of additive hard spheres is used to propose new formulae for the case of disparate-size binary mixtures. A comparison with simulation data and with a recent proposal by Alawneh and Henderson for binary mixtures shows reasonably good agreement with the predictions for the contact values of the large–large radial distribution functions. A discussion on the usefulness and limitations of the new proposals is also presented.

Keywords: hard-sphere mixtures; radial distribution function; contact values

1. Introduction

A well known result in statistical mechanics is the close relationship between the structural and thermodynamic properties of fluids. In the particular case of a multi-component mixture of (additive) hard spheres (HS), the compressibility factor $Z \equiv p/\rho k_{\mathrm{B}} T$ (where p, ρ and T are the pressure, density and temperature of the system and k_{B} is the Boltzmann constant) is given by

$$Z = 1 + 4\eta \sum_{i,j}^{N} \frac{\sigma_{ij}^3}{\langle \sigma^3 \rangle} x_i x_j g_{ij}(\sigma_{ij}), \qquad (1)$$

where N is the number of components in the mixture, x_i is the mole fraction of species i, $\sigma_{ij} = \frac{1}{2}(\sigma_i + \sigma_j)$, σ_i being the diameter of a sphere of species i, $\eta = (\pi/6)\rho \langle \sigma^3 \rangle$ is the packing fraction (with $\langle \sigma^n \rangle \equiv \sum_{i=1}^{N} x_i \sigma_i^n$) and $g_{ij}(\sigma_{ij})$ are the contact values of the radial distribution functions (RDFs) $g_{ij}(r)$. Hence, in this system, knowledge of the contact values of the RDFs suffices to completely determine the equation of state (EOS). Exact results for $g_{ij}(\sigma_{ij})$ are unfortunately only known to first order in the packing fraction, where one simply has

$$g_{ij}(\sigma_{ij}) = 1 + \eta \left(1 + \frac{3}{2} z_{ij}\right) + O(\eta^2), \qquad (2)$$

where

$$z_{ij} \equiv \frac{\sigma_i \sigma_j}{\sigma_{ij}} \frac{\langle \sigma^2 \rangle}{\langle \sigma^3 \rangle}. \qquad (3)$$

Therefore, in general one must rely on either approximations or values obtained from computer simulations. Amongst the most important approximate analytical expressions for the contact values are the ones that follow from the solution of the Percus–Yevick (PY) equation of additive HS mixtures by Lebowitz [1], namely

$$g_{ij}^{\mathrm{PY}}(\sigma_{ij}) = \frac{1}{1-\eta} + \frac{3}{2} \frac{\eta}{(1-\eta)^2} z_{ij}, \qquad (4)$$

and the results obtained from the Scaled Particle Theory (SPT) [2–5],

$$g_{ij}^{\mathrm{SPT}}(\sigma_{ij}) = \frac{1}{1-\eta} + \frac{3}{2} \frac{\eta}{(1-\eta)^2} z_{ij} + \frac{3}{4} \frac{\eta^2}{(1-\eta)^3} z_{ij}^2. \qquad (5)$$

However, neither the PY nor the SPT lead to particularly accurate values and so Boublík [6] and, independently, Grundke and Henderson [7] and Lee and Levesque [8] proposed an interpolation between the PY and the SPT contact values, which we will refer to as the BGHLL values:

$$g_{ij}^{\mathrm{BGHLL}}(\sigma_{ij}) = \frac{1}{1-\eta} + \frac{3}{2} \frac{\eta}{(1-\eta)^2} z_{ij} + \frac{1}{2} \frac{\eta^2}{(1-\eta)^3} z_{ij}^2. \qquad (6)$$

These lead, through Equation (1), to the popular and widely used Boublík–Mansoori–Carnahan–Starling–Leland (BMCSL) EOS [6,9] for HS mixtures. For binary mixtures the BGHLL values are rather accurate except for asymmetric mixtures in which large hard

---

*Corresponding author. Email: andres@unex.es

†On sabbatical leave from Centro de Investigación en Energía, Universidad Nacional Autónoma de México (U.N.A.M.), Temixco, Morelos 62580, Mexico.

spheres are present in extreme dilution in a small hard-sphere solvent. Since such mixtures represent good models for colloidal suspensions and there is growing interest in these kinds of systems, there have been many efforts to correct the deficiencies of the BGHLL values [10–22]. In this paper the recent proposal of [22] is of particular concern, so we also quote it explicitly here. It relies heavily on the proposal of Viduna and Smith (VS) [18] which reads

$$g_{ij}^{VS}(\sigma_{ij}) = \frac{1}{1-\eta} + \eta \frac{3 - \eta + \eta^2/2}{2(1-\eta)^2} z_{ij}$$
$$+ \eta^2 \frac{2 - \eta - \eta^2/2}{3(1-\eta)^3} \left(1 + \frac{\langle\sigma\rangle\langle\sigma^3\rangle}{2\langle\sigma^2\rangle^2}\right) z_{ij}^2. \quad (7)$$

Alawneh and Henderson (AH) [22] restrict themselves to binary mixtures ($N = 2, \sigma_2 \geq \sigma_1$) and propose to keep VS's expression for $g_{11}(\sigma_1)$ but amend $g_{12}(\sigma_{12})$ and $g_{22}(\sigma_2)$ as

$$g_{12}^{AH}(\sigma_{12}) = g_{12}^{VS}(\sigma_{12}) - \frac{\eta^3}{16(1-\eta)^3}(1 - R^{-3})z_{12}^3$$
$$+ \frac{5\eta^4}{32(1-\eta)^3}(1 - R^{-4})z_{12}^4$$
$$- \frac{\eta^5}{16(1-\eta)^3}(1 - R^{-5})z_{12}^5, \quad (8)$$

$$g_{22}^{AH}(\sigma_2) = g_{22}^{VS}(\sigma_2) + \frac{3\eta}{2}(z_{22} - 1)\frac{1 - R^{-1}}{R}$$
$$\times \exp\left[\frac{3\eta}{2}(z_{22} + 1)\right]. \quad (9)$$

Here $R \equiv \sigma_2/\sigma_1$.[1] With these, they get good agreement for the large–small contact values and reasonably good agreement for the large–large contact values as compared to Molecular Dynamics results for mixtures with size ratios going from $R = 1$ to $R = 10$.

On a different vein, in recent papers [23–26] three of us have advocated a 'universality' approach as a guide to propose simple and accurate approximate expressions for the contact values $g_{ij}(\sigma_{ij})$ of additive HS mixtures. In this approach, if the packing fraction η is fixed, the expressions for the contact values of the RDF for all pairs ij of like and unlike species depend on the diameters of both species and on the composition of the mixture *only* through the single dimensionless parameter z_{ij} (cf. Equation (3)), irrespective of the number of components in the mixture. Note that this feature is shared by the PY, SPT and BGHLL results but not by the VS or the AH approximations. The aim of this paper is two-fold. On the one hand, we will assess whether the new simulation data of [22] comply with the universality ansatz. On the other hand, we will introduce a refinement of some of the

simple proposals of [23–26] that retain the universality feature but are able to improve the performance in the case of highly asymmetric mixtures.

The paper is organized as follows. In Section 2 and in order to make the paper self-contained, we provide a rather brief account of the simple proposals based on the universality ansatz and a simple extension to deal with highly asymmetric systems. This is followed in Section 3 by a comparison between the AH contact values, those of the new proposals and the simulation data. The paper is closed in Section 4 with further discussion and some concluding remarks.

2. Proposals for contact values including the 'universality' assumption

We start by recalling the main aspects of the 'universality' approach that has been used recently [23–26] as a guide to propose simple and accurate approximate expressions for the contact values $g_{ij}(\sigma_{ij})$ of additive HS mixtures. According to this approach, at a given total packing fraction η, $g_{ij}(\sigma_{ij})$ depends on the size and concentration distributions only through the single parameter z_{ij}:

$$g_{ij}(\sigma_{ij}) = G(\eta, z_{ij}), \quad (10)$$

where the function $G(\eta, z)$ is a common function for all the pairs (i, j), regardless of the composition and number of components of the mixture. Note that the exact contact values to first order in density (cf. Equation (2)) are consistent with the ansatz (10) with $G(\eta, z) \to 1 + \eta(1 + \frac{3}{2}z)$.

In order to propose specific forms for $G(\eta, z)$ use is made of three basic consistency conditions. First, in the limit in which one of the species, say i, is made of point particles (i.e. $\sigma_i \to 0$), $g_{ii}(\sigma_i)$ must take the ideal gas value, except that one has to take into account that the available volume fraction is $1 - \eta$. Thus,

$$\lim_{\sigma_i \to 0} g_{ii}(\sigma_i) = \frac{1}{1-\eta}. \quad (11)$$

Next, if all the species have the same size, $\{\sigma_k\} \to \sigma$, the system becomes equivalent to a single component system, so that

$$\lim_{\{\sigma_k\} \to \sigma} g_{ij}(\sigma_{ij}) = g_p(\eta), \quad (12)$$

where $g_p(\eta)$ is the contact value of the RDF of the single component fluid at the same packing fraction η as that of the mixture.

The third condition is the equality between the pressure in the bulk and near a hard wall [25,26]:

$$1 + 4\eta \sum_{i,j} \frac{\sigma_{ij}^3}{\langle\sigma^3\rangle} x_i x_j g_{ij}(\sigma_{ij}) = \sum_j x_j g_{wj}, \quad (13)$$

where g_{wj} is the wall–particle correlation function at contact. Since a hard wall can be seen as a sphere of infinite diameter [27], the contact value g_{wj} can be obtained from $g_{ij}(\sigma_{ij})$ as

$$g_{wj} = \lim_{\substack{\sigma_i \to \infty \\ x_i\sigma_i^3 \to 0}} g_{ij}(\sigma_{ij}). \tag{14}$$

In the special case of a pure fluid plus a hard wall, Equation (13) becomes

$$\lim_{\substack{\sigma_2 \to \infty \\ x_2\sigma_2^3 \to 0}} g_{12}(\sigma_{12}) = 1 + 4\eta g_p(\eta) \equiv Z_p(\eta), \tag{15}$$

where $Z_p(\eta)$ is the compressibility factor of the pure fluid.

Assuming the validity of the ansatz (10), conditions (11), (12), (13) and (15) become

$$G(\eta, 0) = \frac{1}{1 - \eta}, \tag{16}$$

$$G(\eta, 1) = g_p(\eta), \tag{17}$$

$$1 + 4\eta \sum_{i,j} \frac{\sigma_{ij}^3}{\langle\sigma^3\rangle} x_i x_j G(\eta, z_{ij})$$

$$= \sum_j x_j G(\eta, z_{wj}), \quad z_{wj} \equiv 2\sigma_j \frac{\langle\sigma^2\rangle}{\langle\sigma^3\rangle}, \tag{18}$$

$$G(\eta, 2) = Z_p(\eta), \tag{19}$$

respectively. Conditions (16), (17) and (19) are fulfilled by the quadratic proposal [23,26]

$$G_{e2}(\eta, z) = \frac{1}{1 - \eta} + \left[g_p(\eta) - \frac{1}{1 - \eta}\right] z$$
$$+ \left[\frac{1 - \eta/2}{1 - \eta} - (1 - 2\eta)g_p(\eta)\right] z(z - 1). \tag{20}$$

However, G_{e2} does not satisfy Equation (18) for an arbitrary number of components $N \geq 3$. This is accomplished by a cubic form [24–26]:

$$G_{e3}(\eta, z) = G_{e2}(\eta, z) + (1 - \eta)\left[g_p^{SPT}(\eta) - g_p(\eta)\right]$$
$$\times z(z - 1)(z - 2), \tag{21}$$

where

$$g_p^{SPT}(\eta) = \frac{1 - \eta/2 + \eta^2/4}{(1 - \eta)^3} \tag{22}$$

is the SPT contact value of the pure fluid. The proposals G_{e2} and G_{e3} are very flexible in the sense that they can accommodate any reasonable choice for $g_p(\eta)$. In particular if $g_p(\eta) = g_p^{SPT}(\eta)$ then $G_{e2}(\eta, z) = G_{e3}(\eta, z)$ and one recovers the SPT contact values given in Equation (5).

Taking either the $g_p(\eta)$ values that follow from the Carnahan–Starling or the Carnahan–Starling–Kolafa (CSK) EOS as input, both approximations G_{e2} and G_{e3} yield in general very good predictions for $g_{ij}(\sigma_{ij})$ in binary and polydisperse mixtures under a wide range of conditions [23–26], which typically implies $z_{ij} \leq 2$. However, in the case of very disparate mixtures, the parameter z_{ij} can take larger values. For instance, in a binary mixture with $R > 1$ one has

$$z_{22}(x_2, R) = R\frac{1 - x_2 + x_2 R^2}{1 - x_2 + x_2 R^3}. \tag{23}$$

The behaviour of z_{22} as a function of $1/R$ is shown in Figure 1 for different values of x_2. It follows that, at fixed x_2, there exists a value $R = R_{max}(x_2)$ at which z_{22} reaches a maximum $z_{22}^{max}(x_2)$. The peak $z_{22}^{max}(x_2)$ becomes narrower and higher as x_2 decreases, its location moving to the left (larger values of R). An explicit expression for $R_{max}(x_2)$ can be derived by differentiation of z_{22} with respect to R, which yields a cubic equation for R whose real solution is

$$R_{max}(x_2) = \frac{1}{2}\left[1 + \left(2x_2^{-1} + 2x_2^{-1}(1 - x_2)^{1/2} - 1\right)^{1/3}\right.$$
$$\left. + \left(2x_2^{-1} + 2x_2^{-1}(1 - x_2)^{1/2} - 1\right)^{-1/3}\right]. \tag{24}$$

A plot of $R_{max}(x_2)$ and the associated values of $z_{22}^{max}(x_2)$ is shown in Figure 2. In the limit $x_2 \to 0$ one gets $R_{max} \to (2x_2)^{-1/3}$, so that $\lim_{x_2 \to 0} x_2 R_{max}^3 = 1/2$. For $x_2 > 0$ one has $x_2 R_{max}^3 > 1/2$. This means that, when z_{22} reaches its maximum value, the partial volume fraction occupied by the big spheres is always larger than half the one occupied by the small ones. Figure 2 shows that $z_{22}^{max}(x_2)$ can reach rather high values for sufficiently small x_2. In particular, $z_{22}^{max}(x_2) > 2$ if $x_2 \leq 0.036$, irrespective of the value of R. Since $G(\eta, z)$ is a monotonically increasing function of z, the larger z_{22}, the higher $g_{22}(\sigma_2)$. Thus, Equation (24) gives the value of R at which $g_{22}(\sigma_2)$ has
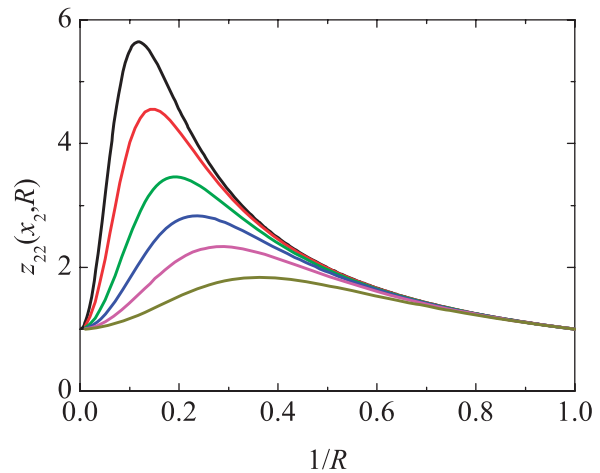

Figure 1. (Colour online). Plot of $z_{22}(x_2)$ as a function of $1/R$ for, from top to bottom, $x_2 = 0.001, 0.002, 0.005, 0.01, 0.02$ and 0.05.

a maximum, according to the ansatz (10). Note that $R^{\max}(x_2)$ is independent of η.

The polynomial forms (20) and (21) are constructed by imposing exact properties at $z=0$, $z=1$ and $z=2$. On the other hand, in disparate mixtures where one can have values of z higher than 2, Equations (20) and (21) are not accurate enough. In fact, again in the binary case, there exists evidence indicating that $g_{22}(\sigma_2)$ grows exponentially for large R, as explicitly incorporated in the AH proposal [22], Equation (9). This translates, in the context of the ansatz (10), into an exponential dependence of $G(\eta, z)$ on z for large z. Thus, here we propose to amend Equations (20) and (21) as

$$G_{e2+}(\eta, z) = \begin{cases} G_{e2}(\eta, z), & 0 \le z \le 2, \\ Z_p(\eta)\exp[A_{e2}(\eta)(z-2)], & 2 \le z, \end{cases} \quad (25)$$

$$G_{e3+}(\eta, z) = \begin{cases} G_{e3}(\eta, z), & 0 \le z \le 2, \\ Z_p(\eta)\exp[A_{e3}(\eta)(z-2)], & 2 \le z, \end{cases}$$
$$\quad (26)$$

where $A_{e2}(\eta)$ and $A_{e3}(\eta)$ are determined by requiring continuity of the first derivative at the matching point $z=2$. Their expressions are

$$A_{e2}(\eta) = \frac{1}{Z_p(\eta)}\left[\frac{2-3\eta/2}{1-\eta} - 2(1-3\eta)g_p(\eta)\right], \quad (27)$$

$$A_{e3}(\eta) = \frac{1}{Z_p(\eta)}\left[\frac{4-9\eta/2+2\eta^2}{(1-\eta)^2} - 4(1-2\eta)g_p(\eta)\right]. \quad (28)$$

Note that the amended proposals (25) and (26) also share with Equations (20) and (21) the flexibility to accommodate any reasonable choice for g_p. In what

follows we will use the one corresponding to the CSK EOS, namely

$$g_p^{\text{CSK}}(\eta) = \frac{1-\eta/2+\eta^2(1-2\eta)/12}{(1-\eta)^3}. \quad (29)$$

3. Comparison with simulation data

Once the new universal proposals have been introduced, the question now arises as to whether the available simulation data are consistent with the universality ansatz. Were this to be the case, for a given packing fraction η plots of g_{ij} versus z_{ij} of different mixtures should lie on a common curve and this will be tested next.

The approximations $G_{e2}(\eta, z)$, $G_{e3}(\eta, z)$, $G_{e2+}(\eta, z)$ and $G_{e3+}(\eta, z)$, given in Equations (20), (21), (25) and (26), respectively, complemented with the CSK expression for $g_p(\eta)$ given in Equation (29), are compared with simulation data of $g_{ij}(\sigma_{ij})$ [22], [28] in Figures 3–6. We can observe that G_{e2} and G_{e3} perform very well for $0 < z < 2$, except for the higher values of $g_{22}(\sigma_2)$ in that region (see the insets of Figures 3–6). Since, by construction, both G_{e2} and G_{e3} give the correct value at $z=2$ (cf. Equation (19)), the deviations of the simulation values of $g_{22}(\sigma_2)$ from the theoretical curves in the region $0 < z < 2$ can be interpreted as
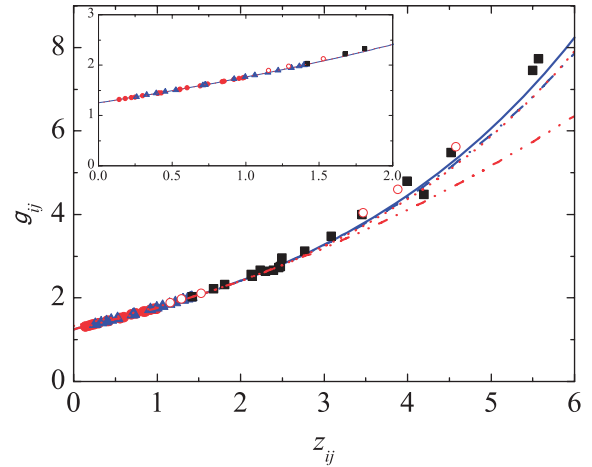
Figure 3. Plot of $g_{ij}(\sigma_{ij})$ as a function of z_{ij} for $\eta = 0.2$. Dash-dot-dot line: $G_{e2}(\eta, z)$; dash-dot line: $G_{e3}(\eta, z)$; dotted line: $G_{e2+}(\eta, z)$; solid line: $G_{e3+}(\eta, z)$; solid circles: simulation data of $g_{11}(\sigma_1)$ from [22]; solid triangles: simulation data of $g_{12}(\sigma_{12})$ from [22]; solid squares: simulation data of $g_{22}(\sigma_2)$ from [22]; open circles: simulation data of g_{w1} and g_{w2} from [28]. The inset shows the region $0 \le z_{ij} \le 2$. Note that $G_{e2+}(\eta, z)$ and $G_{e3}(\eta, z)$ are practically indistinguishable at this density.
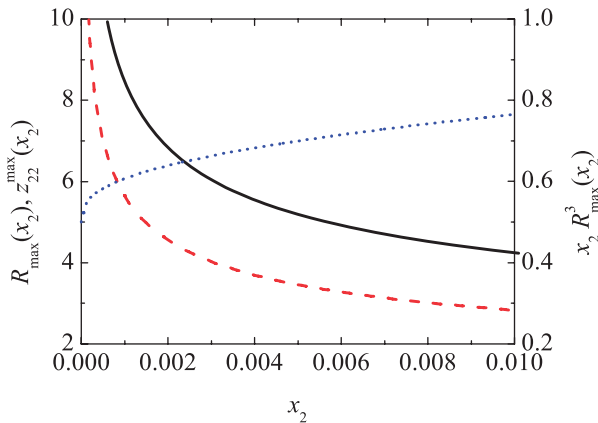

Figure 2. Plot of $R_{\max}(x_2)$ (solid line) and the corresponding $z_{22}^{\max}(x_2)$ (dashed line). Also shown is the behaviour of the quantity $x_2 R_{\max}^3$ (dotted line, right vertical scale) as a function of x_2.

a manifestation of the approximate character of the universality ansatz (10). This seems to be confirmed by the scatter of the simulation data of $g_{22}(\sigma_2)$ for $z > 2$. On the other hand, the overall behaviour of $g_{22}(\sigma_2)$ in that region seems to be reasonably well captured by both G_{e2+} and G_{e3+}.

Once the question of universality has been examined, in order to complement the perspective of the present results, in Figures 7–10 we illustrate some other issues. In particular, we want to assess the performance of the theoretical approximations obtained with the universality assumption, denoted by $g_{22}^*(\sigma_2)$ (where the asterisk will be either $e2, e3, e2+$ or $e3+$ depending on whether one uses $G_{e2}(\eta, z)$, $G_{e3}(\eta, z)$, $G_{e2+}(\eta, z)$ or $G_{e3+}(\eta, z)$, respectively, to compute the contact value) and that of the AH approximation $g_{22}^{AH}(\sigma_2)$

(cf. Equation (9)) as compared to simulation data. Hence, in Figure 7 we have plotted $g_{22}(\sigma_2)$ as a function of $1/R$ taking $x_2 = 0.002$ and $\eta = 0.4$, while in Figure 8 the large–large contact value has been plotted as a function of x_2 for $\eta = 0.4$ and $R = 5$. These plots suggest that the new approximations may indeed improve the already reasonable agreement between the AH formula and simulation results, but all theories seem to underestimate the height of the peak in the $g_{22}(\sigma_2)$ versus $1/R$ plot. The region of interest, namely relatively large R and small x_2,
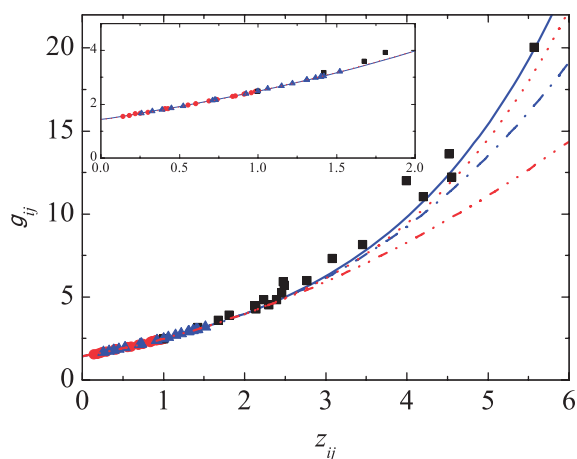

Figure 4. Same as in Figure 3, but for $\eta = 0.3$. At this density there are no simulation data for g_{wj}.
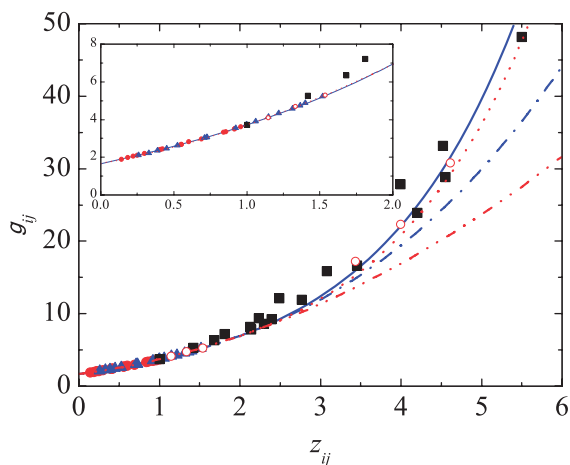

Figure 5. Same as in Figure 3, but for $\eta = 0.4$.

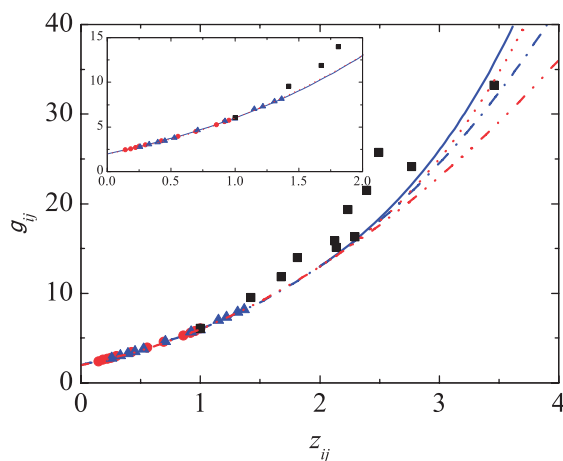
Figure 6. Same as in Figure 3, but for $\eta = 0.5$. At this density there are no simulation data for g_{wj}.
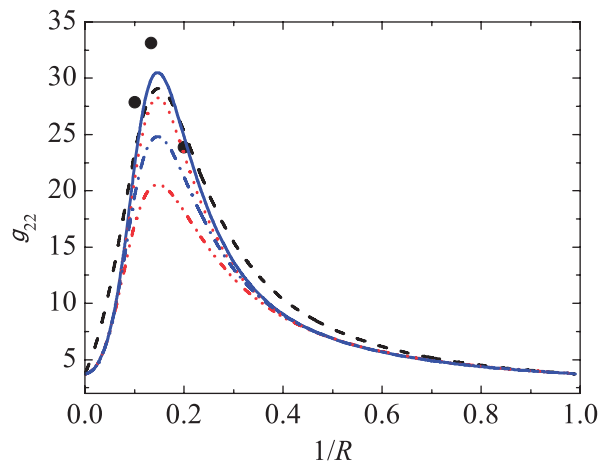

Figure 7. Plot of $g_{22}(\sigma_2)$ as a function of $1/R$ for $\eta = 0.4$ and $x_2 = 0.002$ (as given by different approximations) and simulation results from [22]. Dash-dot-dot line: $g_{22}^{e2}(\sigma_2)$; dash-dot line: $g_{22}^{e3}(\sigma_2)$; dotted line: $g_{22}^{e2+}(\sigma_2)$; solid line: $g_{22}^{e3+}(\sigma_2)$; dashed line: $g_{22}^{AH}(\sigma_2)$; solid circles: simulation data of $g_{22}(\sigma_2)$ from [22].
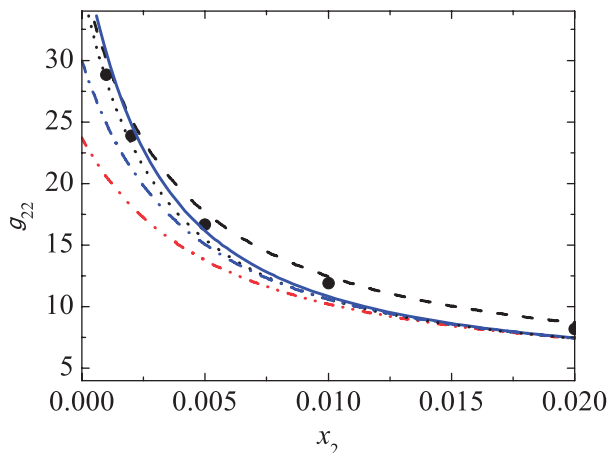
Figure 8. Plot of $g_{22}(\sigma_2)$ as a function of x_2 for $\eta=0.4$ and $R=5$ (as given by different approximations) and simulation results from [22]. Dash-dot-dot line: $g_{22}^{e2}(\sigma_2)$; dash-dot line: $g_{22}^{e3}(\sigma_2)$; dotted line: $g_{22}^{e2+}(\sigma_2)$; solid line: $g_{22}^{e3+}(\sigma_2)$; dashed line: $g_{22}^{AH}(\sigma_2)$; solid circles: simulation data of $g_{22}(\sigma_2)$ from [22].
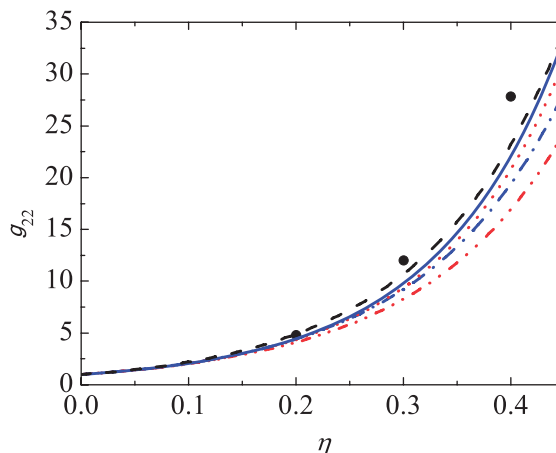

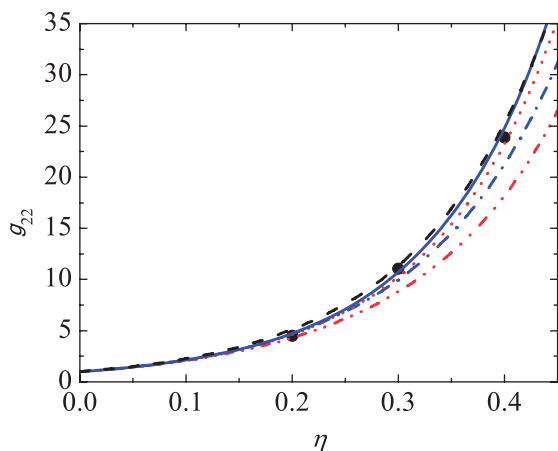Figure 10. Same as in Figure 9, but for $x_2=0.002$ and $R=10$.

Figure 9. Plot of $g_{22}(\sigma_2)$ as a function of η for $x_2 = 0.002$ and $R=5$ (as given by different approximations) and simulation results from [22]. Dash-dot-dot line: $g_{22}^{e2}(\sigma_2)$; dash-dot line: $g_{22}^{e3}(\sigma_2)$; dotted line: $g_{22}^{e2+}(\sigma_2)$; solid line: $g_{22}^{e3+}(\sigma_2)$; dashed line: $g_{22}^{AH}(\sigma_2)$; solid circles: simulation data of $g_{22}(\sigma_2)$ from [22].

is further examined in Figures 9 and 10 which illustrate two additional points. On the one hand, one can clearly see that the curves are almost indistinguishable for low densities (up to $\eta \simeq 0.2$ in these cases) but at higher densities the new proposals $G_{e2+}(\eta, z)$ and $G_{e3+}(\eta, z)$ indeed improve on the performance of the earlier ones $G_{e2}(\eta, z)$ and $G_{e3}(\eta, z)$. On the other hand, they also show that, in the high density region, the AH formula performs a little bit better than either $G_{e2+}(\eta, z)$ or $G_{e3+}(\eta, z)$ as R becomes larger.

4. Concluding remarks

The above results deserve some further consideration. In this paper, following the universality approach that some of us have followed for some years, we have introduced two new proposals [cf. Equations (25) and (26)] for the contact values of HS mixtures which improve on the earlier proposals in the case where one has disparate size mixtures. These proposals fulfill certain exact conditions and are rather flexible, requiring as their only input the contact value of the one-component system.

The comparison with recent computer simulation data [22,28] indicates that the universality assumption may have some limitations but, since there are many technical difficulties in simulating mixtures with large R and very small x_2, one cannot reach definite conclusions on this issue on the basis of these limited data. On the other hand, the new proposals following the universality assumptions for the large–large contact values seem nevertheless to yield reasonably good agreement both with the simulation results and with the recent proposal by Alawneh and Henderson [22].

It is clear that the AH formulae do not obey the ansatz (10). First, the non-universal character of Equation (7) is due to the appearance of the combination $\langle \sigma \rangle \langle \sigma^3 \rangle / \langle \sigma^2 \rangle^2$. In addition, the values given by Equations (8) and (9) depend on $1 - R^{-n}$. As mentioned above, our analysis of the universality issue in the light of the simulation results suggests that the ansatz (10) may break down at some point and hence whether the AH proposal is universal or not would not be particularly relevant. However, a more serious problem with the AH formulae is that Equation (9) fails to reduce to the exact result to first order in η given in Equation (2). In contrast, all

the universal approximations quoted in this paper as well as the VS approximation yield such result in the appropriate limit. Whether or not the universality feature is confirmed or discarded depends on the availability of further simulation results. Our hope is that this paper may encourage the performance of such simulations.

Acknowledgements

Note

1. Note the typographical error in Equation (7) of [22] where a factor of R is missing in the prefactor of the exponential correction to the VS formula.

References

[1] J.L. Lebowitz, Phys. Rev. A **133**, 895 (1964).
[2] H. Reiss, H.L. Frisch, and J.L. Lebowitz, J. Chem. Phys **31**, 369 (1959); E. Helfand, H.L. Frisch, J.L. Lebowitz, J. Chem. Phys. **34**, 1037 (1961); J.L. Lebowitz, E. Helfand and E. Praestgaard, J. Chem. Phys. **43**, 774 (1965).
[3] M.J. Mandell and H. Reiss, J. Stat. Phys **13**, 113 (1975).
[4] Y. Rosenfeld, J. Chem. Phys **89**, 4272 (1988).
[5] M. Heying and D.S. Corti, J. Phys. Chem. B **108**, 19756 (2004).
[6] T. Boublík, J. Chem. Phys **53**, 471 (1970).
[7] E.W. Grundke and D. Henderson, Mol. Phys **24**, 269 (1972).
[8] L.L. Lee and D. Levesque, Mol. Phys **26**, 1351 (1973).
[9] G.A. Mansoori, N.F. Carnahan, K.E. Starling, and J.T.W. Leland, J. Chem. Phys **54**, 1523 (1971).
[10] D. Henderson, A. Malijevský, S. Labík, and K.Y. Chan, Mol. Phys **87**, 273 (1996).
[11] D.H.L. Yau, K.-Y. Chan, and D. Henderson, Mol. Phys. **88**, 1237 (1996); **91**, 1137 (1997).
[12] D.V. Matyushov and B.M. Ladanyi, J. Chem. Phys. **107**, 5815 (1997).
[13] D. Henderson and K.Y. Chan, J. Chem. Phys. **108**, 9946 (1998); Mol. Phys. **94**, 253 (1998); **98**, 1005 (2000).
[14] D. Henderson, D. Boda, K.Y. Chan, and D.T. Wasan, Mol. Phys. **95**, 131 (1998).
[15] D. Matyushov, D. Henderson, and K.-Y. Chan, Mol. Phys. **96**, 1813 (1999).
[16] D. Cao, K.-Y. Chan, D. Henderson, and W. Wang, Mol. Phys. **98**, 619 (2000).
[17] C. Barrio and J.R. Solana, J. Chem. Phys. **113**, 10180 (2000).
[18] D. Viduna and W.R. Smith, Mol. Phys. **100**, 2903 (2002); J. Chem. Phys. **117**, 1214 (2002).
[19] D. Henderson, A. Trokhymchuk, L.V. Woodcock, and K.-Y. Chan, Mol. Phys. **103**, 667 (2005).
[20] A. Vrabecz and G. Tóth, Mol. Phys. **104**, 1843 (2006).
[21] A. Takhtoukh and C. Regnaut, Fluid Phase Equil. **262**, 149 (2007).
[22] M. Alawneh and D. Henderson, Mol. Phys. **106**, 607 (2008).
[23] A. Santos, S.B. Yuste, and M. López de Haro, J. Chem. Phys. **117**, 5785 (2002).
[24] A. Santos, S.B. Yuste, and M. López de Haro, J. Chem. Phys. **123**, 234512 (2005).
[25] M. López de Haro, S.B. Yuste, and A. Santos, Mol. Phys. **104**, 3461 (2006).
[26] M. López de Haro, S.B. Yuste, and A. Santos, *Alternative Approaches to the Equilibrium Properties of Hard-Sphere Liquids,* in *Theory and Simulation of Hard-Sphere Fluids and Related Systems, in the series Lectures Notes in Physics, Vol. 753*, edited by A. Mulero (Springer, Berlin, 2008), pp. 183–245.
[27] D. Henderson, F.F. Abraham, and J.A. Barker, Mol. Phys. **31**, 1291 (1976).
[28] A. Malijevský, S.B. Yuste, A. Santos, and M. López de Haro, Phys. Rev. E **75**, 061201 (2007).